




Preparation of a quantum degenerate mixture of ^{23}Na ^{40}K molecules and ^{40}K atoms

Jin Cao,^{1,2} Huan Yang ,^{1,2} Zhen Su,^{1,2} Xin-Yao Wang,^{1,2} Jun Rui ,^{1,2,3} Bo Zhao ,^{1,2,3} and Jian-Wei Pan^{1,2,3}

¹*Hefei National Research Center for Physical Sciences at the Microscale and School of Physical Sciences, University of Science and Technology of China, Hefei 230026, China*

²*Shanghai Research Center for Quantum Science, CAS Center for Excellence in Quantum Information and Quantum Physics, University of Science and Technology of China, Shanghai 201315, China*

³*Hefei National Laboratory, University of Science and Technology of China, Hefei 230088, China*



(Received 20 August 2022; accepted 5 January 2023; published 17 January 2023)

We report on the preparation of a quantum degenerate mixture of ^{23}Na ^{40}K molecules and ^{40}K atoms. A deeply degenerate atomic mixture of ^{23}Na and ^{40}K atoms with a large number ratio ($N_F/N_B \approx 6$) is prepared in a large-volume optical dipole trap. About 3.0×10^4 ^{23}Na ^{40}K ground-state molecules are created through magnetoassociation followed by stimulated Raman adiabatic passage. The pure molecular gas is in the moderately degenerate regime. In the atom-molecule mixture, the elastic collisions provide a thermalization mechanism for the molecules. The calculated thermalization time constant is smaller than the lifetime of the molecules in the atom-molecule mixture. This indicates that the molecules may reach thermal equilibrium due to elastic atom-molecule collisions before notable losses take place. In a few tens of milliseconds, the degeneracy of the molecules is maintained. This time interval is long enough for the study of strongly interacting atom-molecule mixtures and the production of ultracold triatomic molecular gases.

DOI: [10.1103/PhysRevA.107.013307](https://doi.org/10.1103/PhysRevA.107.013307)

Ultracold molecules have attracted great interest due to their potential applications in the study of chemical reactions at nearly absolute zero temperatures, quantum simulation of exotic models in condensed-matter physics, and precision measurements [1–3]. Recently, magnetic tunable atom-molecule Feshbach resonances have been observed in elastic and inelastic collisions between ^{23}Na ^{40}K molecules and ^{40}K atoms [4–7], and reactive collisions between ^{23}Na ^6Li molecules and ^{23}Na atoms [8]. The analysis in Ref. [6] suggests that the Feshbach resonances are universal features in atom-molecule collisions. Therefore, these Feshbach resonances render atom-molecule mixtures a new platform for quantum simulation and ultracold chemistry. For example, a strongly interacting atom-molecule mixture can be used to study a new type of impurity problem, i.e., angulon [9,10]. The bound states that are associated with the atom-diatomic-molecule Feshbach resonances are triatomic molecular bound states, and, thus, an ultracold atom-diatomic-molecule mixture may be used to create a dense sample of triatomic molecules [11,12]. Besides, the fermionic atom-diatomic-molecule mixture may be used to study novel many-body pairing mechanisms and the fermionic triatomic-molecular superfluids [13]. However, many of these applications require the preparation of a quantum degenerate atom-molecule mixture, which remains elusive.

Although the techniques of preparing quantum degenerate gas of atoms are well established, the creation of quantum degenerate gas of molecules is very difficult. Recently, various diatomic molecules have been created via ultracold association [14–22] and direct laser cooling [23–26]. However, only two groups can create quantum degenerate gas

of molecules [27–30]. In the experiment at the JILA group [27], a deeply degenerate Bose-Fermi mixture of ^{87}Rb and ^{40}K atoms with a large number imbalance is prepared to form the ^{87}Rb ^{40}K molecules in a conventional optical dipole trap. For a large number ratio of $N_F/N_B \approx 7$ with N_B (N_F) the number of bosonic (fermionic) atoms, the spatial mismatch of density between Bose-Einstein condensates (BEC) and degenerate Fermi gases (DFG) is mitigated, and, thus, a high efficiency of association of molecules can be achieved. In the experiment at the MPQ group [29], a deeply degenerate Bose-Fermi mixture of ^{23}Na and ^{40}K atoms with a small number imbalance ($N_F/N_B \approx 3$) is prepared. To form molecules with a high efficiency, a species-dependent dipole trap is used to achieve density matching between BEC and DFG.

To prepare a quantum degenerate mixture of ^{23}Na ^{40}K molecules and ^{40}K atoms, the formation of molecules in a deeply degenerate mixture of ^{23}Na and ^{40}K atoms with a large number imbalance is desired, since it does not require the complicated species-dependent dipole trap, and the Feshbach molecules can be quickly transferred to the ground state once formed. However, it is challenging to prepare a deeply degenerate mixture of ^{23}Na and ^{40}K atoms with a large number imbalance because the three-body loss rate between ^{23}Na and ^{40}K is about ten times larger than that between ^{87}Rb and ^{40}K [29]. Another difficulty in the study of atom-molecule mixtures is that the molecules usually suffer from losses due to collisions with the atoms. Different mechanisms may contribute to the losses, such as photoexcitation by trap lasers, inelastic collisions, and sticky collisions [31–36]. In the mixtures, the elastic collisions must be faster than the inelastic

collisions so that the collisional interactions can be studied before notable losses take place.

In this paper, we report on the preparation of a quantum degenerate mixture of ^{23}Na ^{40}K molecules and ^{40}K atoms. We first prepare a deeply degenerate mixture of ^{23}Na and ^{40}K atoms with a large number imbalance ($N_F/N_B \approx 6$) with $T/T_F \approx 0.2\text{--}0.25$ at a temperature of about 120 nK. About 4.3×10^4 ^{23}Na ^{40}K Feshbach molecules can be formed by adiabatic magnetoassociation. For a typical stimulated Raman adiabatic passage (STIRAP) efficiency of 70%, about 3.0×10^4 ^{23}Na ^{40}K ground-state molecules can be prepared. The two-dimensional (2D) column density distribution of the molecules is fit to the Fermi-Dirac distribution with $T/T_F \approx 0.4\text{--}0.5$. By selectively removing ^{23}Na atoms, we obtain a quantum degenerate mixture of ^{23}Na ^{40}K molecules and ^{40}K atoms. In the atom-molecule mixture, the elastic collisions provide a thermalization mechanism for the molecules. The estimated thermalization time constant is smaller than the lifetime of the molecules in the atom-molecule mixture by approximately one order of magnitude. This indicates that the molecules may reach thermal equilibrium due to elastic atom-molecule collisions before notable losses occur. After a few tens of milliseconds which is larger than the typical thermalization time, the momentum distribution of the molecules can still be fit to the Fermi-Dirac distribution with $T/T_F \approx 0.5\text{--}0.6$. This indicates that the low entropy of the molecular gas can be maintained in the mixture.

Our experiment starts with the preparation of a deeply degenerate mixture of ^{23}Na and ^{40}K atoms. The experimental setup has been introduced in previous works [5,37]. We first load ^{23}Na and ^{40}K atoms into a two-species dark-spot magneto-optical trap. The atoms are optically pumped to the $|f, m_f\rangle_{\text{Na}} = |2, 2\rangle$ state and the $|f, m_f\rangle_{\text{K}} = |9/2, 9/2\rangle$ state and are then loaded into a cloverleaf-type magnetic trap to perform evaporative cooling of ^{23}Na atoms, and the ^{40}K atoms are sympathetically cooled. After that, the atomic mixtures are loaded into a horizontal dipole trap formed by two elliptical laser beams ($\lambda = 1064$ nm) with beam waists of about 38×152 μm crossed at an angle of about 5° . The axial direction of the horizontal dipole trap is along the axial direction of the magnetic trap to ensure mode matching with the cigar-shaped magnetic trap. In this horizontal dipole trap, ^{23}Na atoms are transferred to the $|1, 1\rangle$ state. A vertical dipole trap ($\lambda = 1064$ nm) with a beam waist of approximately 235 μm is adiabatically ramped up to load the ^{23}Na and ^{40}K atoms into a large-volume dipole trap formed by the three laser beams. Optical evaporative cooling is performed in the large-volume three-beam optical dipole trap. At the end of the optical evaporation, we typically create 6.2×10^4 ^{23}Na atoms with a BEC fraction of about 80% and about 3.9×10^5 ^{40}K atoms with a temperature of about 120 nK and $T/T_F \approx 0.2\text{--}0.25$. The absorption images of the quantum degenerate atomic mixture are shown in Fig. 1. The trap frequencies for ^{40}K atoms are $(\omega_x, \omega_y, \omega_z) = 2\pi \times (240, 69, 24)$ Hz. Such a deeply degenerate atomic mixture of ^{23}Na and ^{40}K atoms with a large number ratio ($N_F/N_B \approx 6$) serves as an ideal starting point for the creation of quantum degenerate gas of molecules.

It is worth mentioning that in our paper, we do not implement gray molasses on atoms. In Refs. [27,29], both the JILA and MPQ groups implemented the gray molasses to improve

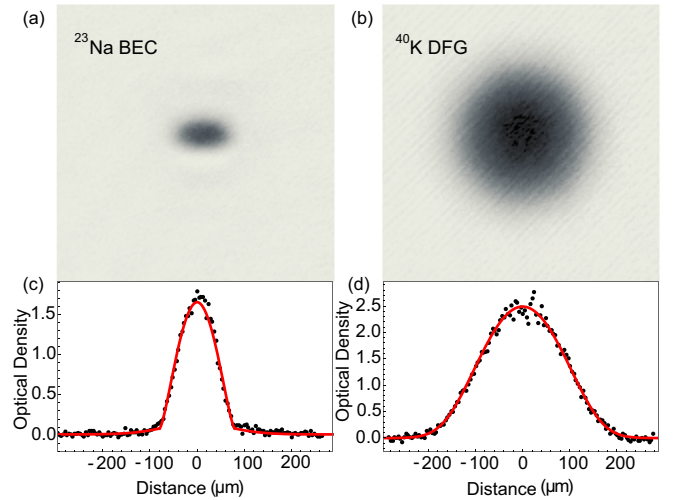


FIG. 1. (a) and (b) Absorption images (average of five images) of a deeply degenerate Bose-Fermi mixture of ^{23}Na and ^{40}K atoms with a large number imbalance after a time-of-flight expansion of 13 ms. (c) and (d) Center-sliced column density. The solid lines in (c) and (d) are bimodal and Fermi-Dirac fitting curves for ^{23}Na and ^{40}K , respectively. The mixture contains about 6.2×10^4 ^{23}Na atoms with a Bose-Einstein condensate fraction of about 80% and about 3.9×10^5 ^{40}K atoms with $T/T_F = 0.24$.

the initial phase-space density of the atoms. It was one of the key techniques for the preparation of a deeply degenerate mixture of ^{87}Rb atoms and ^{40}K atoms with a large number imbalance at the JILA group [27]. Our paper demonstrates that mode-matching loading from the magnetic trap into an optical dipole trap and evaporative cooling in a large-volume dipole trap can be used to prepare a deeply degenerate Bose-Fermi mixture with a large number ratio, even if the mixture has a large three-body loss rate.

After the preparation of the degenerate atomic mixture, we use the Feshbach resonance between the $|1, 1\rangle$ and $|9/2, -7/2\rangle$ states at about 89.8 G to form ^{23}Na ^{40}K Feshbach molecules. To this end, we first transfer the ^{40}K atoms to the $|9/2, -5/2\rangle$ state by a Landau-Zener passage at 32 G. We then ramp the magnetic field to 93 G and transfer the ^{40}K atoms to the $|9/2, -7/2\rangle$ state by a π pulse. The ^{23}Na ^{40}K Feshbach molecules are created by ramping the magnetic field from 93 to 89.5 G at a rate of about 3 G/ms. We typically create about 4.3×10^4 ^{23}Na ^{40}K Feshbach molecules. The number of Feshbach molecules is determined by dissociating the Feshbach molecules into the $|1, 1\rangle + |9/2, -9/2\rangle$ state, and the ^{40}K atoms in the $|9/2, -9/2\rangle$ state are detected by absorption imaging. The efficiency of molecule creation for ^{23}Na atoms is about 70%. Note that this high association efficiency may be overestimated because the thermal components of the ^{23}Na atoms are difficult to discern for a nearly pure BEC and, thus, the number of ^{23}Na atoms may be underestimated.

In the experiment by the MPQ group [29], high efficiency creation of ^{23}Na ^{40}K Feshbach molecules can only be achieved by using a species-dependent optical dipole trap. However, we can achieve a high molecule creation efficiency in a conventional optical dipole trap, which is similar to the formation of ^{87}Rb ^{40}K molecules by the JILA group. This

may be because the large number ratio ($N_F/N_B \approx 6$) in our paper is close to that used in the JILA group ($N_F/N_B \approx 7$) [27]. As pointed out in Refs. [27,38], a large ratio of the number of fermionic atoms to bosonic atoms can help to mitigate the spatial density mismatch and suppress the three-body losses. In addition, the large volume dipole trap in our experiment also reduces the density of the atoms and, thus, can further suppress the three-body losses.

After the Feshbach molecules are created, we transfer the molecules to the rovibrational ground state by STIRAP. We prepare the $^{23}\text{Na } ^{40}\text{K}$ molecules in the hyperfine level $|v, N, m_{i_{\text{Na}}}, m_{i_{\text{K}}}\rangle = |0, 0, -3/2, -3\rangle$ of the ground state, where v and N represent the vibrational and rotational quantum numbers, and $m_{i_{\text{Na}}}$ and $m_{i_{\text{K}}}$ denote the nuclear spin projections of ^{23}Na and ^{40}K , respectively. The σ^- -polarized pump laser and the σ^+ -polarized Stokes laser propagate along the direction of the magnetic field. For a typical STIRAP efficiency of 70%, we create about 3.0×10^4 ground-state molecules. To characterize the degeneracy of the $^{23}\text{Na } ^{40}\text{K}$ molecules, we remove the remaining ^{23}Na atoms and ^{40}K atoms by resonant light pulses. No atoms can be detected after applying the removal pulses. After a short hold time, we transfer the ground-state molecules back to the Feshbach state for detection. The Feshbach molecules are detected by direct absorption imaging.

We find that STIRAP excites the collective modes due to the misalignment and the differences of the trap frequencies. The dominant collective modes are the dipole modes along the x direction and the breathing modes in both the x and the y directions (Fig. 2). Due to the lack of a thermalization process, the collective oscillations can only be damped by the anharmonicity of the dipole trap. The $1/e$ time constants of the damping of the dipole oscillation and the breathing mode along the x direction are 46(12) and 19(4) ms, respectively. No notable damping is observed for the breathing mode along the y direction. After a hold time of about 50 ms, the breathing mode along the x direction is damped whereas the breathing mode along the y direction remains. We then measure the 2D column density distribution of the molecules for a time of flight of 9 ms. The 2D column density distribution of the molecules is fit to the Fermi-Dirac distribution with the fugacity being a fitting parameter. The degeneracy parameter T/T_F is obtained from the fitted fugacity and is shown in Fig. 2. For a hold time of larger than 50 ms, we obtain $T/T_F \approx 0.4$ –0.5.

Since STIRAP conserves the shape of the molecular cloud, this value reflects the degeneracy of the Feshbach molecules. This value is smaller than the degeneracy parameter of $T/T_F \approx 0.6$ calculated from the number of Feshbach molecules and the trap frequencies. This may be because the ^{23}Na atoms are localized at the center of the ^{40}K atoms, and the molecules are dominantly created from the low-entropy part of the deeply degenerate Fermi gas [27]. Therefore, the Feshbach molecules inherit the low entropy of the ^{40}K atoms. STIRAP introduces additional holes in the particle distribution due to the limited efficiency and, thus, reduces the degeneracy of the molecules. The effective degeneracy parameter of the ground-state molecules may be estimated from the modified peak occupancy [39]. For $T/T_F \approx 0.4$ –0.5 and a STIRAP efficiency of 70%, the effective degeneracy parameter is 0.5–0.7. However, a thermalization process is

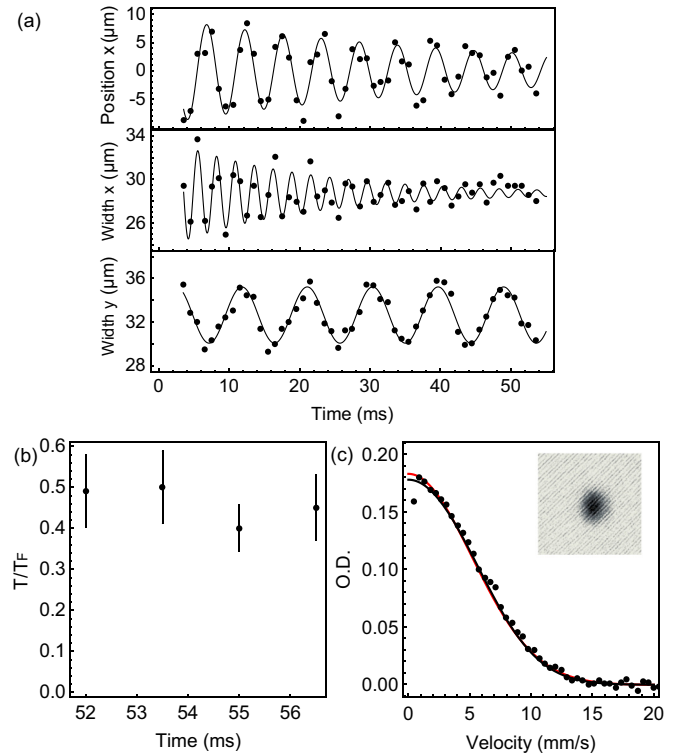


FIG. 2. (a) The collective modes of the molecules induced by STIRAP. The center-of-mass position of the x direction and the widths of the molecular clouds along the x and y directions oscillate as a function of hold time. The $1/e$ time constants of the damping of the dipole oscillation and the breathing mode along the x direction are 46(12) and 19(4) ms, respectively. No notable damping is observed for the breathing mode along the y direction. (b) The degeneracy parameter T/T_F of the $^{23}\text{Na } ^{40}\text{K}$ molecules after a hold time of larger than 50 ms. The 2D column density distribution (average of 10–12 absorption images) is fit to the Fermi-Dirac distribution, and T/T_F is determined from the fitted fugacity. (c) The azimuthal averaged momentum distribution for a hold time of 56.5 ms. The azimuthal averaging is applied after the fitting of the 2D column density distribution. The solid lines are the fit to the Fermi-Dirac distribution (black curve) and the Gaussian distribution (red curve). The inset shows the absorption images (average of ten images) after a time-of-flight expansion of 9 ms. Error bars represent the standard error.

required for the ground-state molecules to reach thermal equilibrium.

After characterizing that the pure molecular gas is in the moderate degenerate regime, we prepare a quantum degenerate mixture of approximately 3×10^4 $^{23}\text{Na } ^{40}\text{K}$ molecules and approximately 3×10^5 ^{40}K atoms at a temperature of about 120 nK by selectively removing the ^{23}Na atoms.

The elastic collisions between $^{23}\text{Na } ^{40}\text{K}$ molecules and ^{40}K atoms provide a thermalization mechanism for the molecules. It is difficult to directly measure the thermalization process in the quantum degenerate atom-molecule mixture due to the collective oscillations. Therefore, we measure the elastic collision sections in a classical mixture using the cross-species thermalization process in Ref. [7]. We start from a mixture of about 380 nK, and heat the atoms to about 850 nK

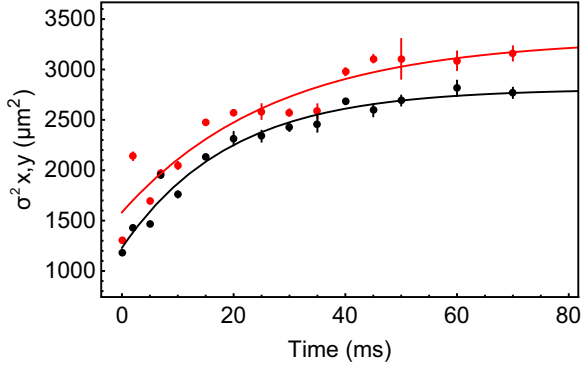


FIG. 3. The thermalization of the $^{23}\text{Na } ^{40}\text{K}$ molecules due to the atom-molecule elastic collisions after heating the ^{40}K atoms. The squares of the molecular cloud sizes σ_x^2 (red) and σ_y^2 (black) are plotted as a function of the hold time. The solid lines are the fits of the data points to exponential functions $\sigma_{x,y}^2 = A_{x,y}e^{-\Gamma_{x,y}t} + B_{x,y}$ where the parameters A , B , and Γ are the fitting parameters. The mean thermalization rate $\Gamma_{\text{th}} = (\Gamma_x + \Gamma_y)/2$ is used to calculate the elastic-scattering cross section. Error bars represent the standard error of the mean.

by a resonant light pulse. The heating pulse also reduces the number of atoms by about a factor of 3. As shown in Fig. 3, the thermalization process can be observed from the change in the sizes of the molecular clouds. The elastic-scattering cross section may be obtained using the formula $\Gamma_{\text{th}} = \Gamma_{\text{coll}}/(3/\xi)$, where Γ_{th} is the thermalization rate and $\Gamma_{\text{coll}} = n_{\text{ov}}\sigma_{\text{el}}v_{\text{rel}}$ is the elastic collision rate [39–41]. Here, n_{ov} is the overlap density, v_{rel} is the relative mean velocity, and the parameter $\xi = 4m_{\text{NaK}}m_{\text{K}}/(m_{\text{NaK}} + m_{\text{K}})^2$ represents the mass effect. Therefore, we have $n_{\text{ov}} = (N_{\text{NaK}} + N_{\text{K}})[(\frac{2\pi k_{\text{B}}T_{\text{K}}}{m_{\text{K}}\omega_{\text{K}}^2})(1 + \frac{m_{\text{K}}T_{\text{NaK}}}{m_{\text{NaK}}T_{\text{K}}\gamma^2})]^{-3/2}$ with $\gamma \approx 0.77$ being the ratio between the trap frequencies for $^{23}\text{Na } ^{40}\text{K}$ molecules and ^{40}K atoms and $v_{\text{rel}} = \sqrt{(8k_{\text{B}}/\pi)(T_{\text{K}}/m_{\text{K}} + T_{\text{NaK}}/m_{\text{NaK}})}$. We obtain $\sigma_{\text{el}} = 6.4(12) \times 10^{-11} \text{ cm}^2$.

The thermalization time constant in the degenerate mixture may be estimated from the elastic-scattering cross sections. If we neglect the Pauli-blocking effects in the quantum degenerate mixture, the thermalization timescale can be estimated using the above formula. For $T/T_{\text{F}} > 0.2$, the Gaussian distribution is a good approximation for calculating $n_{\text{ov}}v_{\text{rel}}$ [42]. Therefore, for $T_{\text{NaK}} = T_{\text{K}} = 120 \text{ nK}$, $N_{\text{K}} = 3.0 \times 10^5$ and $N_{\text{NaK}} = 3.0 \times 10^4$, we obtain $\tau_{\text{th}} \approx 7 \text{ ms}$. Besides the elastic collisions, there are also inelastic collisions in the quantum degenerate atom-molecule mixture. The $1/e$ lifetime of the molecules in the mixtures is about 85 ms, which is about one order of magnitude larger than the estimated thermalization time constant.

The elastic collisions also provide a damping mechanism to the collective modes. The damping of the collective oscillations of the molecules by the atom-molecule elastic collisions is shown in Fig. 4. All the modes are damped due to the atom-molecule elastic collisions. The $1/e$ time constants of the damping of the dipole oscillation along the x direction and the breathing modes along the x and y directions are 17(2), 8(2), and 28(6) ms, respectively. The time constants for damping of the dipole oscillations and the breathing mode along the x direction are reduced by

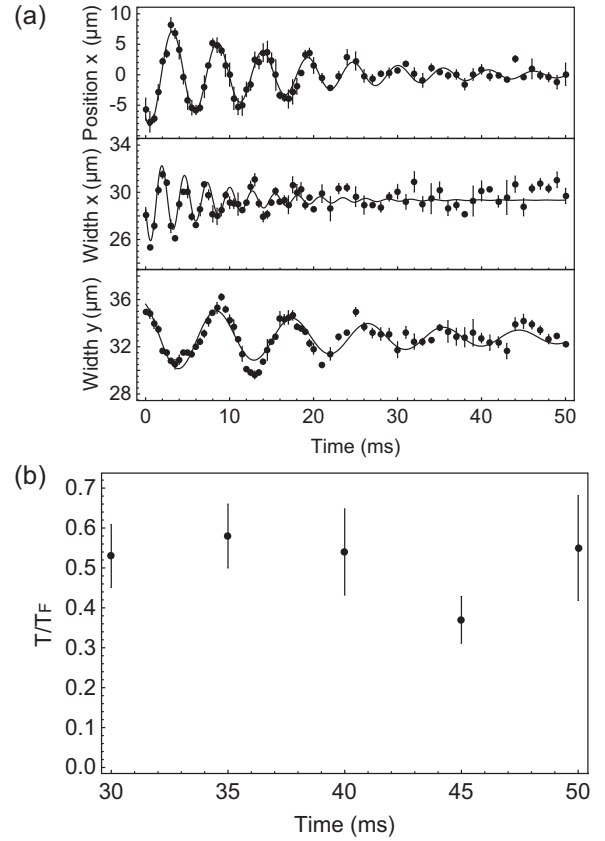


FIG. 4. (a) The damping of the collective modes caused by the elastic collisions between $^{23}\text{Na } ^{40}\text{K}$ molecules and ^{40}K atoms. The $1/e$ time constants of the damping of the dipole oscillation along the x direction and the breathing modes along the x and y directions are 17(2), 8(2), and 28(6) ms, respectively. (b) The degeneracy parameter T/T_{F} of the $^{23}\text{Na } ^{40}\text{K}$ molecules in the atom-molecule mixture for a hold time of 30–50 ms. The 2D column density distribution (average of 20–30 images) is fit to the Fermi-Dirac distribution, and the T/T_{F} is determined from the fitted fugacity. Error bars represent the standard error.

approximately a factor of 2, compared with the damping of pure molecular gases induced by the anharmonicity of the trap. The breathing mode along the y direction is also damped out. From the damping of the dipole oscillations, we may obtain the elastic collision cross sections in the quantum degenerate mixture [39]. The damping rate of the dipole oscillations may be expressed in terms of the elastic collision rate as $1/\tau_{\text{d}} - 1/\tau_0 = (2m_{\text{K}}N_{\text{K}}\Gamma_{\text{coll}})/[3(m_{\text{K}} + m_{\text{NaK}})(N_{\text{K}} + N_{\text{NaK}})]$, where $\tau_{\text{d}} = 17$ and $\tau_0 = 46 \text{ ms}$ are the measured $1/e$ time constants of damping of the dipole oscillations with and without atoms, respectively. We obtain an elastic-scattering cross section $2.7(5) \times 10^{-11} \text{ cm}^2$. This value is smaller than that measured using the thermalization method in a classical mixture. This may be caused by the systematic errors due to different models. The possible Pauli-blocking effects might also cause the suppression of the elastic collisions in a quantum degenerate mixture [42,43]. In our experiment, the atoms are in the deeply degenerate regime, and the molecules are in the moderately degenerate regime. However, it is difficult to measure this effect because

we cannot directly measure the thermalization process in the degenerate mixture.

We measure the degeneracy parameter of the molecules in the atom-molecule mixture for a hold time of 30–50 ms (Fig. 4). This timescale is larger than the damping time of the collective oscillations and the estimated thermalization time but smaller than the lifetime of the molecules in the mixture. We find that the 2D column density distribution can still be fit to the Fermi-Dirac distribution with $T/T_F \approx 0.5$ – 0.6 . These degeneracy parameters are close to the effective degeneracy parameters estimated from the modified peak occupancy. However, they are smaller than the degeneracy parameters $T/T_F \approx 0.8$ – 1 calculated from the trap frequencies and ground-state molecule numbers. This indicates complete thermalization process may need a longer time than the thermalization time constant that the simple thermalization model predicts. On the timescale of a few tens of milliseconds, the degeneracy of the molecules can be maintained, which is favorable for the study of the quantum degenerate atom-molecule mixtures.

To summarize, we have prepared a quantum degenerate mixture of ^{23}Na ^{40}K molecules and ^{40}K atoms. The method of preparing the degenerate molecules in our paper may be useful to other atomic mixtures that also have large three-body loss rates. The collective oscillations induced by the STIRAP lasers can be suppressed by using one-dimensional optical

lattices [27] and optimizing the alignment. Further increasing the degeneracy may be achieved by selectively removing the high-energy ^{40}K atoms and using the atom-molecule elastic collisions to perform evaporative cooling. There are many Feshbach resonances between ^{23}Na ^{40}K molecules and ^{40}K atoms. The Feshbach resonances may be used to improve the thermalization in the mixture by optimizing the ratio of elastic collisions to inelastic collisions. The preparation of the quantum degenerate mixture with tunable interactions paves the way toward studying strongly interacting atom-molecule mixtures, quantum simulation of fermionic angulon [9,10], and preparation of triatomic molecular gases [11,12,44]. The mixture may also be used to study the BCS pairing of atoms and molecules, similar to the ultracold mixture of mass-imbalanced fermionic atoms [45,46].

This work was supported by the National Key R&D Program of China (under Grant No. 2018YFA0306502), the National Natural Science Foundation of China (under Grants No. 12241409, No. 11904355, and No. 12274393), the Chinese Academy of Sciences, the Anhui Initiative in Quantum Information Technologies, the Shanghai Municipal Science and Technology Major Project (Grant No. 2019SHZDZX01), the Shanghai Rising-Star Program (Grant No. 20QA1410000), the Innovation Program for Quantum Science and Technology (Grant No. 2021ZD0302101).

-
- [1] R. V. Krems, *Phys. Chem. Chem. Phys.* **10**, 4079 (2008).
 [2] G. Quémener and P. S. Julienne, *Chem. Rev.* **112**, 4949 (2012).
 [3] L. D. Carr, D. DeMille, R. V. Krems, and J. Ye, *New J. Phys.* **11**, 055049 (2009).
 [4] H. Yang, D.-C. Zhang, L. Liu, Y.-X. Liu, J. Nan, B. Zhao, and J.-W. Pan, *Science* **363**, 261 (2019).
 [5] H. Yang, X.-Y. Wang, Z. Su, J. Cao, D.-C. Zhang, J. Rui, B. Zhao, C.-L. Bai, and J.-W. Pan, *Nature (London)* **602**, 229 (2022).
 [6] X.-Y. Wang, M. D. Frye, Z. Su, J. Cao, L. Liu, D.-C. Zhang, H. Yang, J. M. Hutson, B. Zhao, C.-L. Bai *et al.*, *New J. Phys.* **23**, 115010 (2021).
 [7] Z. Su, H. Yang, J. Cao, X.-Y. Wang, J. Rui, B. Zhao, and J.-W. Pan, *Phys. Rev. Lett.* **129**, 033401 (2022).
 [8] H. Son, J. J. Park, Y.-K. Lu, A. O. Jamison, T. Karman, and W. Ketterle, *Science* **375**, 1006 (2022).
 [9] R. Schmidt and M. Lemesko, *Phys. Rev. Lett.* **114**, 203001 (2015).
 [10] R. Schmidt and M. Lemesko, *Phys. Rev. X* **6**, 011012 (2016).
 [11] T. Köhler, K. Góral, and P. S. Julienne, *Rev. Mod. Phys.* **78**, 1311 (2006).
 [12] R. Hermsmeier, J. Klos, S. Kotochigova, and T. V. Tscherbul, *Phys. Rev. Lett.* **127**, 103402 (2021).
 [13] C. Chin, R. Grimm, P. Julienne, and E. Tiesinga, *Rev. Mod. Phys.* **82**, 1225 (2010).
 [14] K.-K. Ni, S. Ospelkaus, M. H. G. de Miranda, A. Pe'er, B. Neyenhuis, J. J. Zirbel, S. Kotochigova, P. S. Julienne, D. S. Jin, and J. Ye, *Science* **322**, 231 (2008).
 [15] P. K. Molony, P. D. Gregory, Z. Ji, B. Lu, M. P. Köppinger, C. R. Le Sueur, C. L. Blackley, J. M. Hutson, and S. L. Cornish, *Phys. Rev. Lett.* **113**, 255301 (2014).
 [16] T. Takekoshi, L. Reichsöllner, A. Schindewolf, J. M. Hutson, C. R. Le Sueur, O. Dulieu, F. Ferlaino, R. Grimm, and H.-C. Nägerl, *Phys. Rev. Lett.* **113**, 205301 (2014).
 [17] J. W. Park, S. A. Will, and M. W. Zwierlein, *Phys. Rev. Lett.* **114**, 205302 (2015).
 [18] M. Guo, B. Zhu, B. Lu, X. Ye, F. Wang, R. Vexiau, N. Bouloufa-Maafa, G. Quémener, O. Dulieu, and D. Wang, *Phys. Rev. Lett.* **116**, 205303 (2016).
 [19] T. M. Rvachov, H. Son, A. T. Sommer, S. Ebadi, J. J. Park, M. W. Zwierlein, W. Ketterle, and A. O. Jamison, *Phys. Rev. Lett.* **119**, 143001 (2017).
 [20] F. Seeßelberg, N. Buchheim, Z.-K. Lu, T. Schneider, X.-Y. Luo, E. Tiemann, I. Bloch, and C. Gohle, *Phys. Rev. A* **97**, 013405 (2018).
 [21] L. Liu, D.-C. Zhang, H. Yang, Y.-X. Liu, J. Nan, J. Rui, B. Zhao, and J.-W. Pan, *Phys. Rev. Lett.* **122**, 253201 (2019).
 [22] K. K. Voges, P. Gersema, M. Meyer zum Alten Borgloh, T. A. Schulze, T. Hartmann, A. Zenesini, and S. Ospelkaus, *Phys. Rev. Lett.* **125**, 083401 (2020).
 [23] J. F. Barry, D. J. McCarron, E. B. Norrgard, M. H. Steinecker, and D. DeMille, *Nature (London)* **512**, 286 (2014).
 [24] L. W. Cheuk, L. Anderegg, B. L. Augenbraun, Y. Bao, S. Burchesky, W. Ketterle, and J. M. Doyle, *Phys. Rev. Lett.* **121**, 083201 (2018).
 [25] L. Caldwell, J. A. Devlin, H. J. Williams, N. J. Fitch, E. A. Hinds, B. E. Sauer, and M. R. Tarbutt, *Phys. Rev. Lett.* **123**, 033202 (2019).
 [26] S. Ding, Y. Wu, I. A. Finneran, J. J. Bureau, and J. Ye, *Phys. Rev. X* **10**, 021049 (2020).
 [27] L. DeMarco, G. Valtolina, K. Matsuda, W. G. Tobias, J. P. Covey, and J. Ye, *Science* **363**, 853 (2019).

- [28] G. Valtolina, K. Matsuda, W. G. Tobias, J.-R. Li, L. D. Marco, and J. Ye, *Nature (London)* **588**, 239 (2020).
- [29] M. Duda, X.-Y. Chen, A. Schindewolf, R. Bause, J. von Milczewski, R. Schmidt, I. Bloch, and X.-Y. Luo, [arXiv:2111.04301](https://arxiv.org/abs/2111.04301).
- [30] A. Schindewolf, R. Bause, X.-Y. Chen, M. Duda, T. Karman, I. Bloch, and X.-Y. Luo, *Nature (London)* **607**, 677 (2022).
- [31] A. Christianen, M. W. Zwielerlein, G. C. Groenenboom, and T. Karman, *Phys. Rev. Lett.* **123**, 123402 (2019).
- [32] Y. Liu, M.-G. Hu, M. A. Nichols, D. D. Grimes, T. Karman, H. Guo, and K.-K. Ni, *Nat. Phys.* **16**, 1132 (2020).
- [33] P. D. Gregory, J. A. Blackmore, S. L. Bromley, and S. L. Cornish, *Phys. Rev. Lett.* **124**, 163402 (2020).
- [34] M. A. Nichols, Y.-X. Liu, L. Zhu, M.-G. Hu, Y. Liu, and K.-K. Ni, *Phys. Rev. X* **12**, 011049 (2022).
- [35] M. Mayle, B. P. Ruzic, and J. L. Bohn, *Phys. Rev. A* **85**, 062712 (2012).
- [36] M. D. Frye and J. M. Hutson, *New J. Phys.* **23**, 125008 (2021).
- [37] X.-Y. Wang, Z. Su, J. Cao, H. Yang, B. Zhao, C.-L. Bai, and J.-W. Pan, *Sci. China-Phys. Mech. Astron.* **65**, 223011 (2022).
- [38] T. D. Cumby, R. A. Shewmon, M.-G. Hu, J. D. Perreault, and D. S. Jin, *Phys. Rev. A* **87**, 012703 (2013).
- [39] W. G. Tobias, K. Matsuda, G. Valtolina, L. De Marco, J.-R. Li, and J. Ye, *Phys. Rev. Lett.* **124**, 033401 (2020).
- [40] A. Mosk, S. Kraft, M. Mudrich, K. Singer, W. Wohlleben, R. Grimm, and M. Weidemüller, *Appl. Phys. B: Lasers Opt.* **73**, 791 (2001).
- [41] H. Son, J. J. Park, W. Ketterle, and A. O. Jamison, *Nature (London)* **580**, 197 (2020).
- [42] B. DeMarco, S. B. Papp, and D. S. Jin, *Phys. Rev. Lett.* **86**, 5409 (2001).
- [43] B. DeMarco, Ph.D. thesis, University of Colorado, 2001.
- [44] A. Trenkwalder, C. Kohstall, M. Zaccanti, D. Naik, A. I. Sidorov, F. Schreck, and R. Grimm, *Phys. Rev. Lett.* **106**, 115304 (2011).
- [45] C. Ravensbergen, E. Soave, V. Corre, M. Kreyer, B. Huang, E. Kirilov, and R. Grimm, *Phys. Rev. Lett.* **124**, 203402 (2020).
- [46] A. Green, H. Li, J. H. See Toh, X. Tang, K. C. McCormick, M. Li, E. Tiesinga, S. Kotochigova, and S. Gupta, *Phys. Rev. X* **10**, 031037 (2020).